Article Beitr. Phys. Atmosph., August 1994, p. 219–234
0005-8173/94/03 0219–16 $ 3.00/0 Vol. 67, No. 3

Mesoscale Organization and Hailfall Characteristics of Deep Convection in Southern Germany

by H. HÖLLER

Institut für Physik der Atmosphäre, DLR Oberpfaffenhofen, Postfach 1116, 82230 Wessling, Germany

(Manuscript received March 1, 1994; accepted September 6, 1994)

Abstract

This study examines the organization of deep convection on different scales as revealed by radar measurements. The polarimetric parameters allow to discriminate between rain and hail cells. It turned out that hailstorms occur relatively frequent (on 61 % of the thunderstorm days) in an area 200 km in radius around the radar site. On the storm scale the cells were classified as ordinary or single cells, multicells and supercells. In this order of the cell types, a linear decrease in the frequency of occurrence was found. On the meso-β scale a dominance of line structures could be observed. The number of squall lines was non-neglegible.

Zusammenfassung

Mesoskalige Organisation und Hagelcharakteristik hochreichender Konvektion in Süddeutschland

Die aus Radarmessungen abgeleitete Organisation hochreichender Konvektion wird für verschiedene Skalen dargestellt. Mit Hilfe der polarimetrischen Parameter wird eine Unterscheidung von Regen- und Hagelzellen möglich. Es zeigte sich, daß Hagelgewitter in einem Gebiet von 200 km Umkreis um den Radarstandort relativ häufig auftraten (an 61 % der Gewittertage). Auf der Gewitterskala wurden die Zellen als gewöhnliche oder Einzelzellen, Multizellen und als Superzellen klassifiziert. In dieser Reihenfolge der Zellentypen ergab sich eine lineare Abnahme der Häufigkeit ihres Auftretens. Auf der Mesoskala (β) zeigte sich eine Dominanz linienartiger Strukturen. Die Anzahl der 'Squall-Lines' war nicht vernachlässigbar.

1 Introduction

It is well known that deep convection does organize on the mesoscale. This has been demonstrated on the meso-β scale (Houze et al., 1990; Blanchard, 1990) as well as on the meso-γ scale (Marwitz, 1972a, b, c).

On the meso-γ scale (storm scale) severe weather phenomena like hail, downbursts, tornadoes or flooding have been of main interest. From observational studies the different manifestations of the storms could be classified. Three well known archetypal forms of convective cells have been defined (Chisholm and Renick, 1972; Browning, 1977): ordinary (or single) cells, multicellular storms and supercellular storms. Moreover, the severely sheared storm has been introduced by Marwitz (1972c) as a separate category.

Foote (1985) proposed a method of classification using different aspects of the storms: time duration, evolutionary features, or the hail forming processes have been introduced as ordering criteria. It was found that the storm types do not form a discrete hierarchy. Instead, a more or less continuous scale of types exists. The originally defined categories of ordinary, multi- and supercell storms do only represent fixed points of orientation on that scale.

The environmental buoyancy and wind-shear conditions have been recognized as ordering criteria for the cell types. Typical shear conditions have been determined from sounding analysis by Chisholm and Renick (1972) for Alberta storms. Generally, an increase in wind speed and shear was found when proceeding from single cells to multicell and supercell storms. Supercells were also connected with a veering of the wind and shear vectors with height,

whereas for multicell storms the shear was approximately uni-directional (straight line hodograph).

Storm simulations with a three-dimensional cloud model by Weisman and Klemp (1982) refined this picture by the simultaneous consideration of shear and buoyancy. A bulk Richardson number was shown to be a good indicator of storm type: low values correspond to the supercell regime whereas values larger than about 40 represent the multicell regime.

The organization of convection on the larger (meso-β) scale has been classified by Houze et al. (1990) or Blanchard (1990) for Oklahoma storms. Using radar-echo shape, chaotic clusters and line configurations have been recognized. A squall line is a highly organized form of convection. These lines can have a quasi two-dimensional structure and may extend up to a few hundred kilometers in length. Numerical studies by Rotunno et al. (1988) have demonstrated that squall-line longevity is favoured by large amounts of low-level shear.

In this paper the occurrence of the different types of convection in southern Germany is investigated as inferred from radar observations by the DLR polarimetric Doppler radar (Schroth et al., 1988) located in Oberpfaffenhofen near Munich. The frequency of occurrence of the different manifestations of convection in the South German area is of primary interest here. The data reported on have been collected during a six-years period 1987–1992 as part of an observational program focusing on the hail phenomenon (Höller and Meischner, 1990, 1993). Therefore, the microphysical aspects of the precipitation released by the different kinds of cells have been another point of interest. Polarimetric measurements have been shown to provide good indication of hailfall from convective clouds. The differential reflectivity Z_{DR} for linear horizontally or vertically polarized waves has been demonstrated to effectively detect hail below the melting layer (Aydin et al., 1986). The linear depolarization ratio LDR does also indicate hail. This is especially useful in the upper cloud regions above the freezing level (Jameson and Johnson, 1990). These parameters are used here to classify the hail falling from the different types of cells discussed above. Such a combined classification has not yet been performed up to now and will be discussed in this paper for the first time.

The classification scheme used will be discussed in Section 2. In Section 3 the statistics will be presented.

2 The Classification Scheme

2.1 Storm Scale

The manifestation of thunderstorm cells is closely related to the microphysical processes responsible for the formation of precipitation. A cell is defined by closed contours of radar reflectivity which, in turn, is a function of the number concentration, size distribution and thermodynamic phase of the particles envolved. In their developing stages the cells coincide with individual updraft turrets. Later on, reflectivity maxima may also be caused by particle growth in favoured regions of a developed storm circulation, e.g. in the main updraft of a mature thunderstorm.

For the purpose of this study a three-category scheme is adopted classifying the storms as:

SI: ordinary or single cells
M: multicellular storms
S: supercell storms.

It has been recognized (Foote, 1985) that these are more or less archetypal structures representing fixed points on a basically continuous scale of storms. Nevertheless, it is assumed here that these types can be used to represent a whole class of storms having the same basic features in common.

The characteristics of a single-cell storm are shown schematically in Figure 1. The complete cycle of precipitation development and fallout takes place in one cell. Particles are not transferred into another cell (discrete evolution; Foote, 1985). At time t_1 the cell is in its cumulus stage. It exclusively consists of cloud droplets or small ice crystals not yet detectable by radar. At time t_2 a first radar echo has developed due to the presence of rimed ice particles, graupel, snow, or raindrops. The cell now is in its growing stage. Intense riming of these particles resulting in cm-sized hailstones has proceeded at t_3 when the cell enters its mature stage. While the upper part of the cloud is still growing, a first downdraft has formed associated with the fallout of precipitation. At t_4 (decaying stage) the cloud releases its precipitation to the ground in connection with an intensified downdraft (downburst). In the upper part of the storm the updraft air has spread horizontally when reaching equilibrium level forming the typical thunderstorm anvil. If the hailstones are large enough so that they do not melt completely during fallout below the melting level, they can hit the ground and cause damages. But, due to the transient nature of the cell and its relatively low propagation speed, the resulting hailswath at

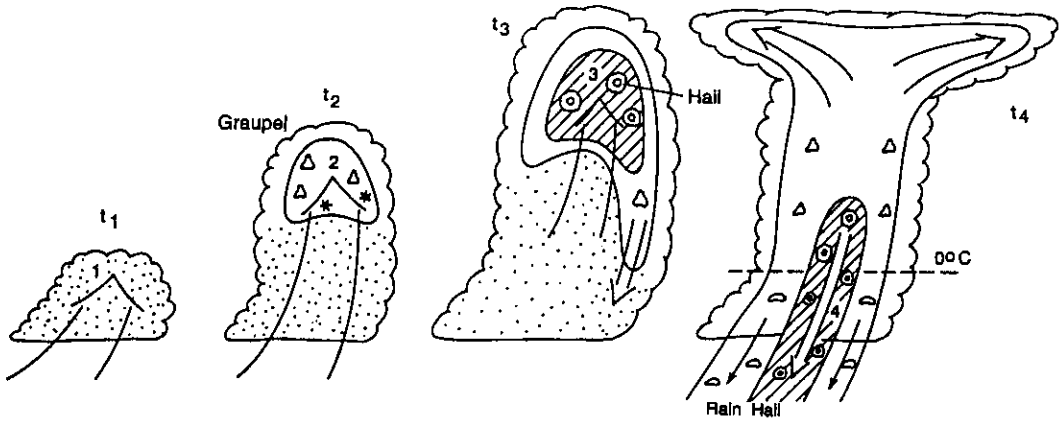

Figure 1 Schematic diagram of a single-cell thunderstorm. Four different stages of cloud development are shown (t_1 through t_4). Graupel is forming at t_2, hail at t_3 and precipitation is falling out of the cloud at t_4. The solid lines indicat contours of radar reflectivity with increasing values towards the cloud's interior.

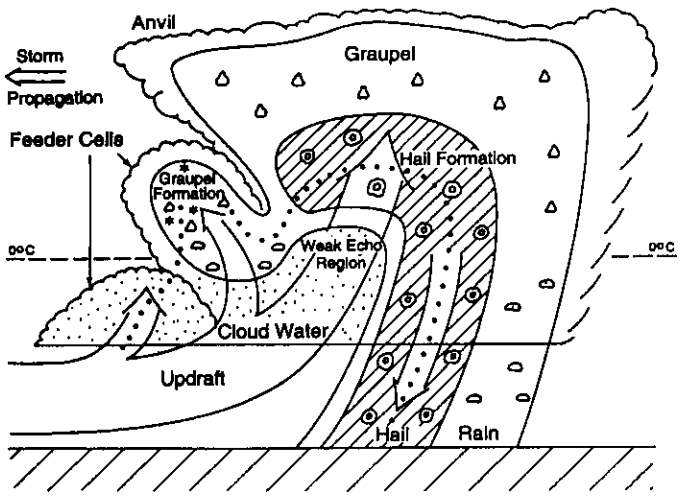

Figure 2 Schematic diagram of a multicell thunderstorm. A succession of cells in different stages of development can be seen contributing to a common cloud mass. Graupel particles are forming in the newly grown cells in the left part of the Figure. Later on, in the mature stage of the cell these graupel can act as hailstone embryos. Hail formation essentially takes place right on top of the weak echo region (WER). The solid lines indicate contours of radar reflectivity with increasing values towards the cloud's interior. The trajectory of an ice nucleus growing into a hailstone is indicated by the dotted line.

the ground is usually small. The duration of the hailfall is only a few minutes. The typical time interval between each consecutive snapshot in Figure 1 is 5 minutes. Single-cell storms either may occur in isolation or they are organized in large-scale complexes or lines. Here they can coexist and interact with other single cells or even multicell or supercell storms.

In multicell storms (Figure 2) cells in all stages of development are coexisting each one forming a part of the same storm system. One large updraft is building the root for the individual towers which become clearly visible in the higher parts of the storm. The hail formation processes are all active permanently, the different stages acting in different cells. In contrast to that, they are active consecutively with time within the single cells. Because of this multicellular structure of the storm, there might exist an exchange of particles among the different cells. Graupel falling in the growing cells (feeder cells) above the low level inflow region can be swept towards the storm's center where they enter the main updraft region. Following such trajectories these particles are recirculated into the storm and start to rise again. In the main updraft they may encounter very high liquid water contents and can grow into large hailstones while crossing the main updraft horizontally. On the downwind side hail particles enter the storm's main downdraft and rapidly fall down to the ground. The processes described here give rise to the typical radar structure of these cells: a forward flank (vault-like) overhang of particles growing into hail on top of a weak echo region (WER) of high liquid-water content (cloud water, usually not detected by radar). Updraft speeds in the WER are too high for graupel or hail particles to penetrate these regions in appreciable amounts. If the storm is developed less intense or if the contributing cells do have a wider spacing, the graupel originating in the feeder clouds may fall out of the cloud before being able to recirculate. A WER does not exist in this case. Hailfalls from such systems are less intense than

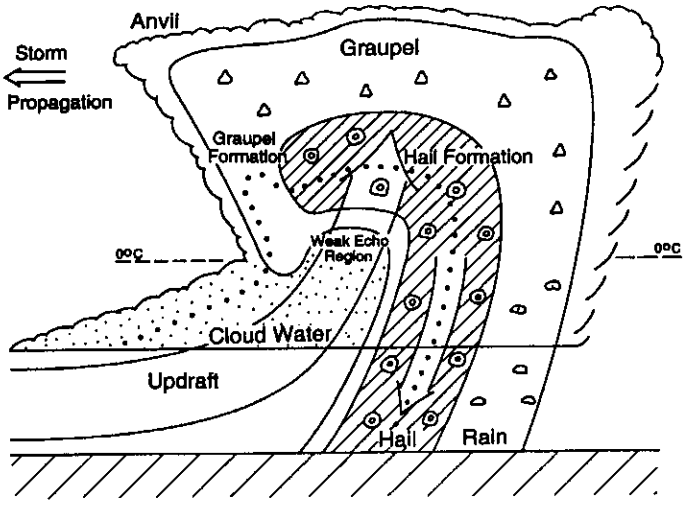

Figure 3 Schematic diagram of a supercell thunderstorm. The storm is formed by a large, quasi-stationary cell. All the different stages of hail formation (particle trajectory indicated by the dotted line) take place within the same cell but at different locations. The solid lines indicate contours of radar reflectivity with increasing values towards the cloud's interior.

those resulting from vaulted multicells. Multicell storms are more persistent than single cells, typically lasting 10 to 60 minutes. The associated hailswaths are in the range 10 to 100 kilometers in length.

Supercell storms are formed by a single large updraft (Figure 3) which does not break up into multiple branches. The graupel particles which later on can grow into hail are formed at the fringes of the updraft zone on the upshear side (with respect to mid-level shear) of the storms. These regions do play the part of the feeder cells in the multicellular case. The subsequent phase of hail growth is basically similar in multicells and supercells, except for the larger updraft size of supercell storms. Supercells have a much higher persistence than the other types of storms. Their quasi-steady structure is maintained for more than half an hour (by definition, see Browning, 1977). These cells can last for several hours, extreme cases of up to 12 hours duration have been reported (Paul, 1973). The corresponding hailswath can extend some hundred kilometers in length. The 'Munich hailstorm' of 12 July 1984 did show such characteristics (Höller and Reinhardt, 1986). The hailswath had a length of about 300 km while ranging between 5 and 10 km in width. Hailstone sizes were extremely large (up to 10 cm in the Munich case).

Between the discrete multicell development and the steady supercells transitional forms of storms can be observed. These storms have been termed weak evolutionary by Foote and Wade (1982) or hydrid storms (Nelson and Knight, 1987; Nelson, 1987). In the present classification scheme these storms are either counted as multicells or as supercells depending on the dominant characteristics.

2.2 Hailfall Characteristics

The characteristics of the hailfalls is inferred from the polarimetric measurements. It has been shown previously that the differential reflectivity Z_{DR} as well as the linear depolarization ratio LDR can successfully be used for hail detection (Bringi et al., 1986a, b).

The differential reflectivity Z_{DR} between horizontally (H) and vertically (V) polarized waves is defined as

$$Z_{DR} = 10 \log (Z_{HH}/Z_{VV})$$

where Z_{HH} and Z_{VV} represent the reflectivity factors for horizontally or vertically transmitted (first index) or received (second index) waves, respectively. Z_{DR} has successfully been used to disriminate rain from hail (Aydin et al., 1986). With increasing size raindrops become more and more oblate, their larger axis being oriented horizontally (Pruppacher and Klett, 1978). This causes Z_{DR} to be positive and to increase with increasing drop size. On the other hand, hail is more irregularly shaped or tumbling. Therefore, Z_{DR} for hail is nearly 0 dB. Occasionally, oblate hail with its major axis oriented vertically can cause even negative values of Z_{DR}. Generally, the reflectivity (Z_{HH} or Z_{VV}) in hail is larger than in rain.

Based on these findings, a hail signal function has been defined by Aydin et al. (1986). This Z_{DR} hail signature is especially useful below the melting level. Small hail or graupel does melt completely before reaching the ground. Z_{DR} is increasing progressively with decreasing height from 0 dB at the melting level to some positive value near the ground. Large hail is able to reach the ground with only incomplete melting during its fallout. This causes Z_{DR} values around 0 dB in the hailshaft extending from the hail formation region aloft all the way down to the ground. Between these two extremes mixed phase precipitation may exist. Raindrops resulting from the melting of small hail can coexist with incompletely melted hail (possibly an ice core surrounded by a water shell). For such a mixture Z_{DR} is in the transitional region from the pure rain values to 0 dB.

Above the melting level the linear depolarization ratio LDR can give good indications for hail regions (Jameson and Johnson, 1990). LDR is defined as

$$LDR = 10 \log (Z_{HV}/Z_{VV})$$

thus reflecting the particles' scattering characteristics perpendicular to the incident wave. Like Z_{DR}, LDR is also depending on the shape and orientation of the particles present in the volume under consideration. In general, LDR typically has higher values for hail as compared to graupel or rain (Aydin et al., 1991; Bringi et al., 1986a, b). Z_{DR} and LDR have been used by Höller et al. (1994) for hydrometeor discrimination in a hailstorm. Different kinds of particles like snow, graupel, rain, hail, or mixtures of rain and ice could be identified. A detailed discussion of the derivation of the classification from scattering calculations was presented.

Depending on the polarimetric parameters described above the following classification of thunderstorm cells is adopted in this paper:

R: Rain cells. All ice particles melt completely reaching the ground as pure rain. Z_{DR} is positive having values typical for rain.

h: Small hail, mostly mixed with rain can be expected at the ground. Hailstones do not exceed sizes of 0.5 to 1 cm in diameter. Z_{DR} is in the intermediate range between rain and hail. Only minor damages may be caused by such hailfalls.

H: Large hail, stones with diameters larger than 1 cm can be expected to hit the ground. Z_{DR} ranges around 0 dB. LDR is relatively high. Such hailfalls can cause considerable damage.

2.3 Mesoscale Organization

In the context of this study the radar-derived meso-β scale organization of convective storms is of interest. The main guideline for classifying the storms is the shape of the radar echo. Four basic configurations have been identified:

I: Isolated storms. Thunderstorms exist more or less isolated and are not embedded in common reflectivity contours. Such isolated storms may appear as singular events or irregularly scattered.

C: Clusters or complexes of storms. Thunderstorms are closely grouped together embedded in a circumscribed reflectivity contour. A variety of clusters might coexist at a given instant at different locations in the observational area. A cluster does not have a preferred direction of alignment (orientation) of the contributing storms.

L: Line-oriented storms. Thunderstorms do have a preferred direction of alignment. They may appear as a line of isolated storms or as a linear complex circumscribed by a common reflectivity contour. The typical maximum dimension should be more than twice as large as the typical minimum dimension. Otherwise the system is classified as a cluster.

SL: Squall lines. This is special form of line-oriented systems. The typical maximum dimension is very large as compared to the typical minimum dimension. The length-to-width ratio is at least five-to-one according to the definition of a mesoscale line (from U.S. Departments of Commerce and Defense, 1980) used by Bluestein and Jain (1985). The length of the line is at least 50 km persisting for at least 15 min. In many cases the system develops a quasi two-dimensional structure. In contrast to the line oriented storms the squall lines are often characterized by a leading line of heavy convection followed by a region of widespread stratiform precipitation.

The classification scheme differs from that introduced by Houze et al. (1990) as it is treating the line systems in less detail. The structures termed isolated storms (I) or clusters (C) can be compared to the chaotic or unclassifiable systems defined by Houze et al. (1990). Line-oriented storms (L) and squall lines (SL) find their counterparts in the weakly or strongly classifiable systems, respectively. In the present study no attempt was made to compare the systems with the leading-line/trailing-stratiform idealization. Moreover, all convective systems observed were considered, whereas Houze et al. (1990) did study only major rain events.

3 Statistics of Radar Measurements

A 'thunderstorm day' (T) is used in this study as a classification unit. It is defined to start at 6 a.m. and lasts until 6 a.m. the next morning. Thereby, an optimum adjustment to the convective time scale is possible. Furthermore, a thunderstorm day is supposed to be a day on which convective cells were either observed by the radar on operational days or could be verified by other means (Weather Service reports). The maximum radar observed range had a radius of 300 km centered at the radar site (Oberpfaffenhofen near Munich). The structural informa-

tion on the far range (200–300 km) was not used for classification purposes (at least in the majority of the cases) because of the limited resolution of the radar measurements (1° beam width). In terms of a quantitative interpretation, the polarimetric measurements for ranges larger than 100 km are no longer reliable for the same reason. Therefore, the number of thunderstorm days is larger than the number of days where hail- or structural classification was possible by the radar measurements.

Different forms of convective organization might occur at different times or even simultaneously at different locations on the same day. As far as the large-scale organization is concerned, all the different types are listed in the Tables. The storm-scale organization does follow a well developed hierarchy extending from the weakly organized single cells to the higher organized multicells and supercell storms. For classificational purposes only those types exhibiting the highest degrees of organization (with increasing order from SI to M and finally S) are listed in the Tables. This implies that SI-storms may have been precursors of the M- or S-storms. On the other hand, S-storms do not necessarily develop from M-storms. A similar type of hierarchy does exist for the hail classification. Rain cells develop into hail cells (h) or even (H). But here a day with large hail (H) may also include h-cells. R-cells did develop on all of the hail days.

The statistics of the thunderstorm days, the hail characteristic as well as the large-scale organization are shown in Tables 1–6 on a day-by-day basis for the period 1987–1992. As noted in the Tables, radar observations are not available for all of the thunderstorm days. Neverthless, if storm or hail reports were available from Weather-Service data, ground based observations at the radar site, or sources of various kinds (like newspapers or insurance companies), the days were classified and included in the Tables. As is shown in the summary (Table 7), this was only done for a few cases for which this information could be obtained reliably. No systematic check of the non-observational days was carried out. Of course, this lack of completeness does reduce the number of cases observed. But, as the present study does focus on the interrelations between mesoscale convective patterns of different types (hail, cell structure, and large scale organization) the complete time series is not required.

It is obvious from Tables 1–6 that the occurrence of thunderstorms is not completely random. It often happens that a period of thunderstorm days is followed by a period of non-thunderstorm days. As

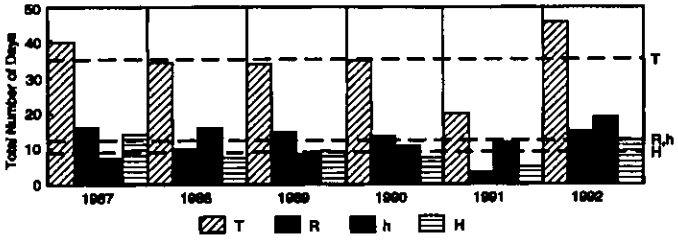

Figure 4 Yearly variation and averages of thunderstorm days (T), days with rain cells only (R), cells producing small hail (h) or large hail (H).

the dataset is not a complete one we do not do statistics of these phenomena. Moreover, we are interested here in the hail and storm type characteristics. But, on the other hand, these missing data are not the cause of the periodicities. These must be attributed to equivalent periodicities in the synoptic conditions providing the large-scale environment for storm development.

Table 7 as well as Figure 4 demonstrate the yearly variation and the average values of thunderstorm days and the hail type. An average of 35 thunderstorm days (T) per year was observed in the 6 years period. The rain cells (R) as well as the small-hail cells (h) both occurred with the same average number of 12 events per year. This corresponds to an averge occurrence of 35 % of the T-days (see Table 8). 9 H-days were observed on average which is 26 % of the T-days. In Table 8 the relative occurrence of the different cell types with respect to the total number of (R + h + H)-days is also shown. Caused by the incomplete classification the results are slightly different from those using T-days as a reference.

The relatively high number of hail days (h or H) might be surprising at first sight. But, keeping in mind the definition of a hail day as a day with at least one hail cell occurring, it is not a measure of the frequency of occurrence of the different cell types. This frequency clearly decreases when proceeding from R to h and finally H-cells as on a h or H-day many R-cells may occur as well. The present result indicates that hailstorms can be observed relatively frequent (at least one per day) on thunderstorm days (on 61 % of the T-days) in an observational area extending about 200 km around the radar site.

In contrast to the hail characteristic, the frequency of the storm types does show a more linearly decreasing order. From Figure 5 we clearly note a decreasing trend in the number of cells from SI to M and finally S-cells. Days where only SI-cells devel-

Table 1 Summary of convective activity in 1987: (T) thunderstorm days, (R) rain cells, cells releasing small (h) or large (H) hail, (SI) single cells, (M) multicells, (S) supercells, (I) mesoscale (β) organization in individual cells, (C) clusters, (L) lines, or (SL) squall lines.

1987

Day	May	June	July	August
1	x		T H M I, SL	
2	x		T R SI	
3	T h x		T R SI	
4	x		T h M	
5	x	T h SI		T R SI
6	x			
7	x		T H M	
8	x		T H SI	
9	x			T H M
10	x			T h SI
11	x			
12	x	T R SI C	T H M	T R SI
13	No	T H S I		
14	Radar	T H S I	T H M	T R M
15	x		T H M	
16	x		T H S SL	
17	x	T h SI	T h SI SL	
18	T H x			T R SI
19	T x			
20	T x	T R SI		
21	x	T R SI	T R M	
22	x	T R SI	T R SI	
23	x		T H M	T H M
24	x		T H M	
25	x		T R SI	
26	x			
27	T h x			
28	T R x			
29	x			
30	x	T R SI	T R SI	
31	x			
Total				
T	6	9	17	7
R	1	5	6	4
h	2	2	2	1
H	1	2	9	2
SI		7	7	4
M			9	2
S		2	1	
I		2	1	
C		1		
L				
SL			3	

Table 2 Summary of convective activity in 1988. Symbols as in Table 1.

1988

Day	May	June	July	August
1			T H M	T h SI
2				T H M L
3		T R M L		T R SI
4				
5			T H M	
6				
7			T R SI L	
8		T	T R SI	
9	T R SI		T R SI	
10		T H M		
11		T R SI		
12		T R SI L	T h SI	
13				
14				
15	T h M L			
16	T h SI I, L			
17	T h SI			
18	T h SI			
19	T h M L	T h SI L, SL		
20				
21				
22			T R SI	
23				
24			T H M SL	
25				T h SI
26	T h SI	T h SI C, L		
27	T H SI	T h SI		
28	T h SI	T h SI C, SL		
29	T H M		T R SI	
30	T h M	T h SI C		
31				
Total				
T	11	10	9	4
R	1	3	5	1
h	8	5	1	2
H	2	1	3	1
SI	7	7	6	3
M	4	2	3	1
S				
I	1			
C		3		
L	3	4	1	1
SL		2	1	

Table 3 Summary of convective activity in 1989. Symbols as in Table 1.

1989

Day	May	June	July	August
1		T R SI	T H M C, L	x
2			T R SI L	x
3				x
4			T	x
5			T h SI L	x
6			T R SI	x
7			T R SI L	x
8		T h SI C	T H M SL	x
9			T R SI L	x
10			T R SI L	x
11				x
12	T H M			x
13				x
14	T H M		T h	x
15			x	No
16			x	Radar
17			x	x
18			x	x
19	T R SI		x	x
20	T R SI		T H x	x
21	T R SI	T h SI	x	x
22		T H M SL	No	x
23	T R SI		Radar	x
24	T R SI	T R SI	x	x
25	T h SI C	T R SI	x	x
26	T R SI C	T H SI C, L	x	x
27	T h SI C, L	T h SI C, L	x	x
28	T R SI L		x	x
29	T h SI C, L		x	x
30	T H M L		x	x
31			T H x	x
Total				
T	13	8	12	
R	7	3	5	
h	3	3	2	
H	3	2	4	
SI	10	7	7	
M	3	11	2	
S				
I				
C	4	3	1	
L	4	2	6	
SL		1	1	

Table 4 Summary of convective activity in 1990. Symbols as in Table 1.

1990

Day	May	June	July	August
1				
2				
3				
4				
5				
6	T			T R SI
7	T h SI L			
8	T R SI			
9	T h SI C, L			
10	T H SI SL			
11	T H M C			
12	T R SI			T h SI L
13	T R SI	T h SI L		T R SI L
14				T R SI C
15	T R SI			
16				T H M C
17	T R SI		T	
18		T h M C, L		
19		T		
20		T H S SL		
21	T R SI L			
22	T R SI			
23	T H M C, L			
24				
25				T h M C
26		T R SI C		T R SI
27		T h M SL		
28		T R SI C, L		T h M C
29		T H M C, SL		T h SI C
30		T H M I, SL	T	T h SI I, L
31			T h SI	
Total				
T	13	9	3	10
R	7	2		4
h	2	3	1	5
H	3	3		1
SI	10	3	1	7
M	2	4		3
S		1		
I		1		1
C	3	4		5
L	4	3		3
SL	1	4		

Table 5 Summary of convective activity in 1991 S ymbols as in Table 1.

1991

Day	May	June	July	August
1		T H M C, L		
2		T R SI		
3		T h SI L		
4				
5				
6				
7		T h SI L	T h SI C	
8			T h SI C	T h SI SL
9			T R SI L	
10			T h SI C	
11				
12			T h M C, L, SL	T h SI C, L
13		T H M L	T h M L	T h SI C
14				T H SI C
15				
16				
17			T H M L, SL	
18				
19				
20				
21				
22		T h SI		
23				
24		T R SI	T h SI SL	
25				
26		T H M L		
27				
28				
29				
30				
31				
Total				
T		8	8	4
R		2	1	
h		3	6	3
H		3	1	1
SI		5	5	4
M		3	3	
S				
I				
C		1	4	3
L		5	4	1
SL			3	1

Table 6 Summary of convective activity in 1992. Symbols as in Table 1.

1992

Day	May	June	July	August
1		T R SI I, L	T H M C, L	T h S C, L
2		T H M C, L, SL	T h SI C, L	T R M C, L
3		T R SI C, L	T h SI C, L	T h M I, C, L
4		T H M C, L	T h M L	
5				
6		T h M C, L	T h SI I, L	
7				T H M C
8		T H M I, C, L		
9		T h SI	T R SI C, L	
10		T H M L	T h SI C, L	T R M C, L
11				
12				
13		T h SI C		
14				
15				
16			T H M C	
17		T R SI	T R SI L	
18				
19				
20		T H SI C, L	T h SI C	T h M C, L
21	T h SI I, C		T H SI L	T H S I, L
22				T R SI L
23	T R SI L	T h SI L		
24	T h SI L	T h SI C	T H SI I	
25	T R SI I	T R SI L		
26	T R SI I, C, L	T R SI L		T H M I, L
27	T h SI L			
28				T R SI C
29			T h SI C	T R SI L
30				
31			T H S I, L	
Total				
T	6	15	14	11
R	3	5	2	5
h	3	5	8	3
H		5	4	3
SI	6	10	10	3
M		5	3	6
S			1	2
I	3	2	3	3
C	2	8	8	7
L	4	11	10	9
SL		1		

Table 7 Yearly average and total number of days for the different storm and hail categories. Symbols as in Table 1. Last line contains unclassified T-days concerning the precipitation (prec.) (R, h, H) and cell (SI, M, S) classifications.

	1987	1988	1989	1990	1991	1992	Average	Total
T	39	34	33	35	20	46	35	207
R	16	10	15	13	3	15	12	72
h	7	16	8	11	12	19	12	73
H	14	7	9	7	5	12	9	54
SI	18	23	24	21	14	29	22	129
M	11	10	6	9	6	14	10	56
S	3	–	–	1	–	3	1	7
h + H	21	23	17	18	17	31	21	127
R + h + H	37	33	32	31	20	46	33	199
SI + M + S	32	33	30	31	20	46	32	192
unclass. prec./cell	2/7	1/1	1/3	4/4	-/-	-/-		

Table 8 Relative number of days for the different storm and hail categories with respect to the thunderstorm days and to days with cell or hail classification. Symbols as in Table 1.

	% T	% (SI + M + S)	% (R + h + H)
R	35		36
h	35		36
H	26		27
h + H	61		64
SI	62	67	
M	28	29	
S	3	4	
SI + M + S	93		

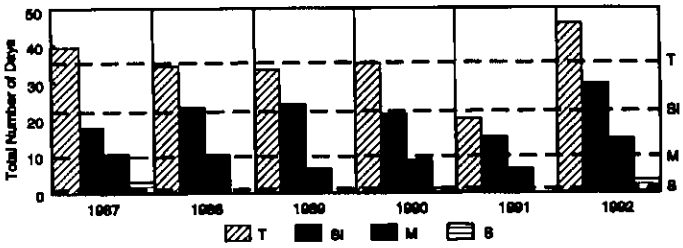

Figure 5 Yearly variation and averages of the number of thunderstorm days (T), days with single cell (SI), multicell (M), and supercell (S) storms.

oped were observed most frequently (67 % of the classifiable days). Multicells occurred in 29 % and supercells in only 4 % of all classified days (differences to 100 % in the total number arise from rounding). Again, this statistics is not indicative of the number of cells occurring but, moreover, for the number of days the special kind of storm could be observed at least once. This implies, that on M as well as on S-days many more single cells (or single cells and multicells in the S-day case) could have been observed.

As pointed out in the previous paragraphs, the hail and cell classifications cause a strong bias towards the larger and more intense classes. Therefore, the statistics is especially useful for assessing the risk of severe weather occurring in the observational area. But it does not allow to directly infer the number of storms of the different types or the area affected by the convection. For example, there are normally a lot of rain cells developing on a day which culminates in small or even large hail. Also several hail cells might be active on the same day or even at the same time, for instance as part of a squall line. Depending on the size, the number, and the life time, these cells do affect a certain part of the total observational domain. All these features are not addressed in the context of this paper but should be considered in a deeper analysis of the data. As far as hail damages are concerned, an assessment of the number of hailstorms and the damages connected with the h and H categories was made by Höller and Meischner (1993). This study also presents the

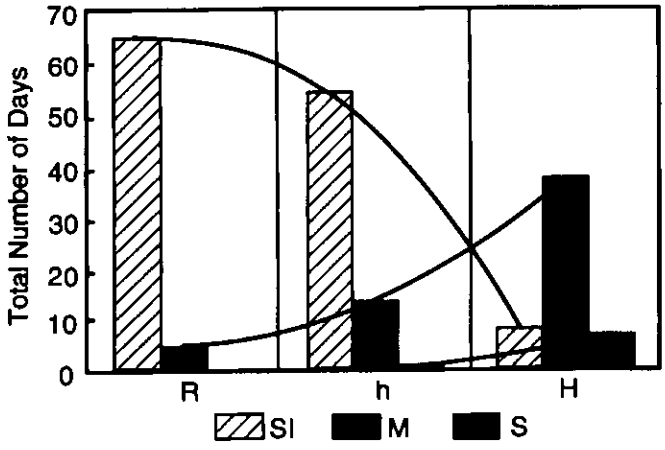

Figure 6 Total number of days with single cells (SI), multicells (M), and supercells (S) in the rain (R), small hail (h), and large hail (H) categories. Possible functional dependencies are indicated by the solid lines.

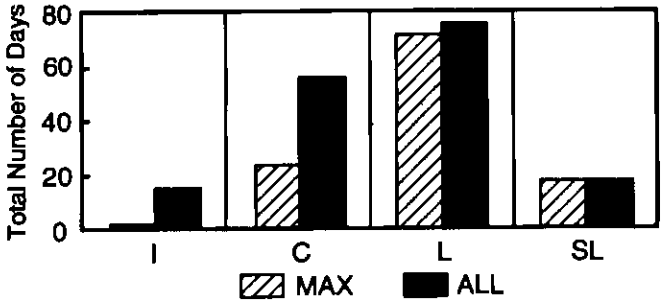

Figure 7 Large scale (meso-β) organization of convection in the 6-years period 1987–1992. Total number of days as a function of convective type: (I) individual cells, (C) cloud cluster, (L) line structures, and (SL) squall lines. MAX: only maximum daily development is counted, ALL: all different types of convection are added.

regional distribution of radar-identified hailfalls defined by certain reflectivity thresholds. Thus it includes the effects of cell size and life-time. Up to 4 haildays per year could be detected locally.

We will now address the question of a possible interdependence of the cell type and the hail type. Such an analysis is shown in Figure 6. We note two different types of dependencies: (1) a decreasing frequency with increasing hail size for single cells, and (2) an increasing number of days for multicells and supercells. In the single cell case the number of the rain and small-hail days is not of significant difference whereas large hail was observed very rarely falling out of these cells. Multicells are preferably associated with hail, the large hail category dominating. This trend is even more pronounced for supercells with a ratio of 6:1 for the H:h-days. On rain days mostly single cells develop. Occasionally, weaker multicells can also not be able to produce hail at the ground. Supercell days have always been hail days. Days with small hail (h) mostly show single cell characteristics, but the contribution of multicell storms is non-negligible. Only one supercell case did result in small hail. The prevailing number of days with large hail (H) is connected to multicell storms. The contribution of single cells is relatively small but comparable to the supercell part.

In spite of the bias introduced by the cell and hail classification scheme the described types of dependencies are still such as we would expect from the definition of the different cell and hail types in Chapter 2: the larger hailfalls are produced in larger cells with increasing magnitude from SI to M and even S-cells. If the total number of cells would have been considered a much stronger decreasing tendency is to be expected for the number of single cells with increasing hail size. This is due to the relatively large number of single cells forming on a thunderstorm day. These are only taken into account by the present classification if no multicells or supercells form on that day. Even then they are only counted as a single event. For the multicells and supercells the cell-hail relation should be similar to the one shown in Figure 6 as the number of cells is much closer to the number of days of occurrence.

Figure 7 presents an overview of the mesoscale (meso-β) organization of the thunderstorms during the observational period. The typical size or length of a convective complex has been used as an ordering criterion. Order increases from the small-scale individual cells (I) to clusters or complexes (C), lines (L) or even squall lines (SL). In Figure 7 two different classification schemes are shown: (MAX) only the highest order convective system is counted per day and (ALL) does also consider multiple structures observed on the same day. The results clearly indicate the dominance of line structures. This especially holds for the MAX-case whereas in the ALL-case the number of clusters is considerably increased but still smaller than the number of lines. We also note a non-negligible number of squall lines (SL). Such lines often produce severe weather phenomena like heavy gusts or hail damages. A case study of such a squall line was presented by Meischner et al. (1991). Considering all observations, individual or isolated storms (I) were observed with about the same frequency as the squall lines.

The preferred formation of line-like structures has also been found by Houze et al. (1990) for Oklaho-

ma rainstorms.Two-thirds of their systems exhibited a moving line structure (corresponding to the L and SL categories in this paper), whereas one-third of the cases had a chaotic, unclassifiable character (corresponding to the I or C categories). The frequency of occurrence is not completely comparable as Houze et al. (1990) did only consider major rainstorms whereas in the present study all convective events have been taken into account.

4 Summary and Conclusions

This paper investigates the mesoscale characteristics of deep convection in southern Germany as revealed by polarimetric and Doppler-radar measurements. The microphysical as well as the cellular and large-scale properties of thunderstorms are reported.

On the microphysical scale the cells were classified as rain cells or hail cells, the latter being further identified as cells producing small or large hail. This type of classification was supported by the polarimetric measurements of differential reflectivity and linear depolarization ratio. It turned out that hailstorms could be observed relatively frequent (on 61 % of the thunderstorm days) in an area 200 km in radius around the radar site.

On the storm scale the cells were classified as ordinary or single cells, multicells, and supercells. In this order of the cell types a linear decrease in the frequency of occurrence was found.

Different types of interdependencies for the cell and hail types were noted: the number of single-cell days was decreasing whereas the number of multicell and supercell days was increasing with hail size. On rain days mostly single cells did develop. This also holds for days with small hail, but the contribution of multicell days can not be neglected. Large hail was mostly connected with multicells.

On the meso-β scale a dominance of line structures was found. The number of squall lines was non-neglegible.

The polarimetric parameters were found to be especially useful for determining the hail and cell-type relations for the south German area. The regional characteristics of the hailfalls could also be determined from the data available. This problem was not in the focus of the present paper but should be addressed in a further study. This also holds for the dependencies of convective phenomena on the 'environmental' conditions like atmospheric stability or wind shear.

Acknowledgements

This study was supported by the County of Rosenheim and the Bavarian Minister for Economy and Traffic.

References

Aydin, K., V. Giridhar and *Y. Zhao,* 1991: Polarimetric C-band radar observables in melting hail: a computational study. 25'th Int. Conf. Radar Meteor., Paris, AMS, 733–736.

Aydin, K., T. A. Seliga and *V. Balaji,* 1986: Remote sensing of hail with a dual linear polarization radar. J. Climate Appl. Meteor. **25,** 1475–1484.

Blanchard, D., 1990: Mesoscale convective patterns of the southern high plains. Bull. Amer. Meteor. Soc. **71,** 994–1005.

Bluestein, H. B. and *M. H. Jain,* 1985: Formation of mesoscale lines of precipitation: Severe squall lines in Oklahoma during spring. J. Atmos. Sci. **42,** 1711–1732.

Bringi, V. N., R. M. Rasmussen and *J. Vivekanandan,* 1986a: Multiparameter radar measurements in Colorado convective storms. Part I: Graupel melting studies. J. Atmos. Sci. **43,** 2545–2563.

Bringi, V. N., J. Vivekanandan and *J. D. Tuttle,* 1986b: Multiparameter radar measurements in Colorado convective storms. Part II: Hail detection studies. J. Atmos. Sci. **43,** 2564–2577.

Browning, K. A., 1977: The structure and mechanisms of hailstorms. In Foote G. B. and C. A. Knight (Eds.): Hail: a review of hail science and hail suppression. Amer. Meteor. Soc., Boston, 1–43.

Chisholm, A. J. and *J. H. Renick,* 1972: The kinematics of multicell and supercell Alberta hailstorms, Alberta hail studies, 1972. Research Council of Alberta hail studies Rep. No. 72-2, 24–31.

Foote, G. B., 1985: Aspects of cumulonimbus classification relevant to the hail problem. J. Rech. Atmos. **19,** 61–74.

Foote, G. B. and *C. G. Wade,* 1982: Case study of a hailstorm in Colorado. Part I: Radar echo structure and evolution. J. Atmos. Sci. **39,** 2828–2846.

Höller, H., V. N. Bringi, J. Hubbert, M. Hagen and *P. F. Meischner,* 1994: Life cycle and precipitation formation in a hybrid-type hailstorm revealed by polarimetric and Doppler radar measurements. J. Atmos. Sci. **51,** 2500–2522.

Höller, H. and *P. F. Meischner,* 1990: Untersuchung von mikro- und makrophysikalischen Strukturen und Prozessen in Hagelwolken im Hinblick auf deren Beeinflußbarkeit (in German). DLR-FB 90-38, 54 pp.

Höller, H. and *P. F. Meischner,* 1993: Untersuchung von mikro- und makrophysikalischen Strukturen und Prozessen in Hagelwolken im Hinblick auf deren Beeinflußbarkeit (in German). DLR-FB 93-25, 68 pp.

*Höller, H.*and *M. E. Reinhardt,* 1986: The Munich hailstorm of July 12, 1984 – Convective development and preliminary hailstone analysis. Beitr. Phys. Atmos. **59,** 1–12.

Houze, R. A., B. F. Smull and *P. Dodge,* 1990: Mesoscale organization of springtime rainstorms in Oklahoma. Mon. Wea. Rev. **118,** 613–654.

Jameson, A. R. and *D. B. Johnson,* 1990: Cloud microphysics and radar. In: Atlas, D. (Ed.): Radar in Meteorology. Amer. Meteor. Soc., Boston, 323–340.

Marwitz, J. D., 1972a: The structure and motion of severe hailstorms. Part I: supercell storms. J. Appl. Meteor. **11,** 166–179.

Marwitz, J. D., 1972b: The structure and motion of severe hailstorms. Part II: multi-cell storms. J. Appl. Meteor. **11,** 180–188.

Marwitz, J. D., 1972c: The structure and motion of severe hailstorms. Part III: severely sheared storms. J. Appl. Meteor. **11,** 189–201.

Meischner, P. F., V. N. Bringi, D. Heimann and *H. Höller,* 1991: A squall line in southern Germany: Kinematics and precipitation formation as deduced by advanced polarimetric and Doppler radar measurements. Mon. Wea. Rev. **119,** 678–701.

Nelson, S. P. and *N. C. Knight,* 1987: The hydrid multicellular-supercellular storm – and efficient hail producer. Part I: An archetypal example. J. Atmos. Sci. **44,** 2042–2059.

Nelson, S. P., 1987: The hybrid multicellular-supercellular storm – an efficient hail producer. Part II: General characteristics and implications for hail growth. J. Atmos. Sci. **44,** 2060–2073.

Paul, A. H., 1973: The heavy hail of 23–24 July 1971 on the Western Prairies of Canada. Weather **28,** 463–471.

Pruppacher, H. R. and *J. D. Klett,* 1978: Microphysics of clouds and precipitation. Reidel Publishing Company, Dordrecht, 714 pp.

Rotunno, R., J. B. Klemp and *M. L. Weisman,* 1988: A theory for strong, long-lived squall lines. J. Atmos. Sci. **45,** 463–485.

Schroth, A. C., M. S. Chandra and *P. F. Meischner,* 1988: A C-band coherent polarimetric radar for propagation and cloud physics research. J. Atmos. Ocean. Tech. **5,** 803–822.

U.S. Depts. of Commerce and Defense, 1980: Weather radar observations Part A. Federal Meteorological Handbook, No. 7, 5-1-5-2.

Weisman, M. L. and *J. B. Klemp,* 1982: The dependence of numerically simulated convective storms on vertical wind shear and buoyancy. Mon. Wea. Rev. **110,** 504–520.